PROCEEDINGS B

royalsocietypublishing.org/journal/rspb

Research

Cite this article: Edie SM, Khouja SC, Collins KS, Crouch NMA, Jablonski D. 2022 Evolutionary modularity, integration and disparity in an accretionary skeleton: analysis of venerid Bivalvia. *Proc. R. Soc. B* **289**: 20211199.
https://doi.org/10.1098/rspb.2021.1199

Received: 1 June 2021
Accepted: 9 December 2021

Subject Category:
Evolution

Subject Areas:
evolution

Keywords:
three-dimensional morphology, integration, modularity, disparity, marine bivalve

Author for correspondence:
Stewart M. Edie
e-mail: edies@si.edu

Electronic supplementary material is available online at https://doi.org/10.6084/m9.figshare.c.5769766.

THE ROYAL SOCIETY PUBLISHING

Evolutionary modularity, integration and disparity in an accretionary skeleton: analysis of venerid Bivalvia

Stewart M. Edie[1], Safia C. Khouja[2], Katie S. Collins[3], Nicholas M. A. Crouch[2] and David Jablonski[2,4]

[1]Department of Paleobiology, National Museum of Natural History, Smithsonian Institution, Washington, DC 20013, USA
[2]Department of the Geophysical Sciences, University of Chicago, 5734 South Ellis Ave, Chicago, IL 60637, USA
[3]Department of Earth Sciences, Invertebrates and Plants Palaeobiology Division, Natural History Museum, London SW7 5BD, UK
[4]Committee on Evolutionary Biology, University of Chicago, Chicago, IL 60637, USA

SME, 0000-0003-2843-7952; KSC, 0000-0002-3379-4201; NMAC, 0000-0002-3504-8245

Modular evolution, the relatively independent evolution of body parts, may promote high morphological disparity in a clade. Conversely, integrated evolution via stronger covariation of parts may limit disparity. However, integration can also promote high disparity by channelling morphological evolution along lines of least resistance—a process that may be particularly important in the accumulation of disparity in the many invertebrate systems having accretionary growth. We use a time-calibrated phylogenetic hypothesis and high-density, three-dimensional semilandmarking to analyse the relationship between modularity, integration and disparity in the most diverse extant bivalve family: the Veneridae. In general, venerids have a simple, two-module parcellation of their body that is divided into features of the calcium carbonate shell and features of the internal soft anatomy. This division falls more along developmental than functional lines when placed in the context of bivalve anatomy and biomechanics. The venerid body is tightly integrated in absolute terms, but disparity appears to increase with modularity strength among subclades and ecologies. Thus, shifts towards more mosaic evolution beget higher morphological variance in this speciose family.

1. Introduction

Integration—the covariation of traits—is often seen as channelling natural selection by limiting the potential directions of evolutionary change, and modularity—the partitioning of trait covariation into modules—as allowing traits to evolve in a more independent manner [1–6]. Thus, clades with high disparity may be composed of taxa with weak, rather than strong, covariation of traits. However, weak covariation does not necessarily create the modularity often held as key to evolutionary lability, and strong integration—i.e. more integrated evolution *sensu* Pigliucci [7]—need not impose low disparity [8]. Most analyses of modularity, integration and disparity have focused on specific components of the vertebrate endoskeleton such as the vertebral column or cranium (e.g. [9,10]), each with discrete elements arising from populations of skeletogenic cells (termed 'fundamental developmental units' in [11]). By contrast, the accretionary exoskeleton of marine bivalves, the shell, is deposited as one unit by specialized tissues along the growth margin [12] and records most components of the animal's body plan. This accretionary growth may impose a highly integrated structure on the organism, potentially limiting modular responses to selection and thus the accumulation of disparity within the clade. Bivalves are emerging as a model system for macroecology and macroevolution [13,14], but the effects of modularity and integration on their

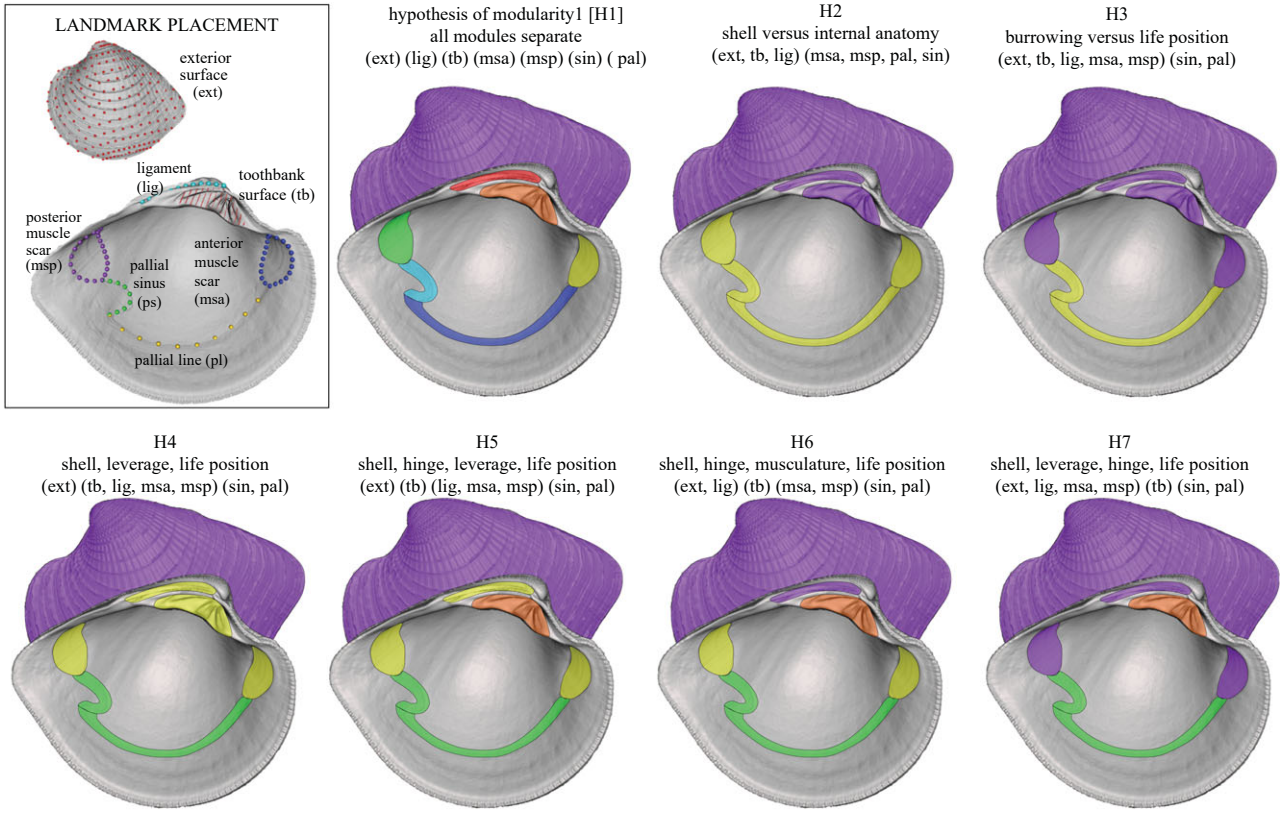

Figure 1. Landmarking scheme for the venerid bivalve shell features and hypotheses of modularity (details in ST§2.1). Colours mark hypothesized modules with shell features grouped by parentheses. Taxon is *Chionopsis amathusia* (Philippi 1844). (Online version is in colour.)

phenotypic evolution remain a major gap in our knowledge of this highly diverse and disparate class [15,16].

Here, we analyse the evolutionary modularity and integration [17] in a phylogenetic and ecological context of the most speciose bivalve family (Veneridae, approximately 750 species [18], analysing 128 of the 134 extant genera). Given the shell's accretionary growth [12], we expect weak modularity and strong integration among its features. However, many shell features are homoplasic across the class, suggesting that mosaic evolution and thus modularity could be an important aspect of bivalve evolution. Notably, the biomechanical demands of shallow- to deep-burrowing, nestling and boring life habits evidently select for particular morphologies [19–21]; for example, deep burrowers tend to have smooth, elongate shells with larger pallial sinuses to accommodate the soft-tissue siphons that maintain contact with the overlying seawater. We therefore expect modularity in the venerid shell to represent 'functional integration' [7,17,22] more than 'developmental integration' [17].

To evaluate modularity structure in venerids, we frame hypotheses for seven *a priori* shell features (figure 1). The most complex hypothesis specifies each feature as a distinct module (H1). Alternatively, features functioning together to achieve a task may covary, i.e. the partitioning of shell features among the components of the bivalve's biomechanical lever arm (adductor muscles, ligament, toothbank and exterior shell surface, see H3–7). Features may also covary according to shared developmental pathways, such as the early separation of cell lineages that give rise to the shell and internal soft anatomy [23] (H2). Modularity structure may also differ among lineages and ecologies, and so we evaluate these hypotheses across the entire family and for phylogenetic and ecological subgroups: the two major subclades (clades 'A' and 'B' after [24], their figure 11), substratum uses across the family and certain substratum uses within subclades. Finally, given the apparent developmental restrictions imposed by the indeterminate, accretionary growth of the bivalve shell, we expect that broad morphological variance (disparity) will be associated with stronger covariation of modules (stronger integration) across the body and also within modules.

2. Methods

(a) Specimen sampling

As in studies of evolutionary integration and modularity in vertebrates [10,25,26], broad phylogenetic and ecological diversity was captured here by sampling representative taxa from lineages (usually a specimen of the type species of its genus). One left valve from an adult individual was sampled per genus in the bivalve family Veneridae (128 of 134 extant genera, and thus 128 of approximately 750 known species; all specimens sampled with permission from museum collections). Venerids are equivalve; left and right valves are largely mirror images except for the offset of their interlocking hinge dentition. Morphological variation among individuals and congeneric species is small relative to among-genus variation in the Veneridae and is unlikely to bias the inferences made here (e.g. [27,28], see also electronic supplementary material, text §1, abbreviated hereafter ST§1). Targeting a single bivalve family also increased the ability to sample homologous structures. Bivalve genera were assigned to a single substratum use (nestling, boring, shallow- or deep-infaunal; [18]). Specimens were scanned using micro-CT at the University of Chicago's Paleo-CT facility. Three-dimensional, isosurface, triangular-mesh models were created in VG Studio Max and cleaned in Rvcg [29] and Meshmixer.

(b) Time-calibrated phylogenetic hypothesis of Veneridae genera

To place analyses in a phylogenetic context, we hypothesized a time-calibrated topology of genera within the Veneridae using genetic data in GenBank, published morphological phylogenies, cladistics and the family's fossil record. The molecular topology was reconstructed by aligning all available sequence data from all venerid species in GenBank (June 2020) using *phylotaR* [30] (ST§2.1), updating the taxonomy of those species and removing dubious tip placements because of erroneous names (two of 174 sequenced species; electronic supplementary material, figure S1, ST§2.2). Of those 174 sequenced species, 59 were sampled for their morphology (= 59 unique genera of the targeted 128). An additional 15 genera forming monophyletic clades were sampled for their morphology using congeneric species, arriving at 74 of 128 genera sampled on the molecular phylogeny (ST§2.3). The remaining 54 genera lacking molecular data were grafted onto the molecular topology using topologies from published morphological phylogenies or cladistic relationships (electronic supplementary material, figure S2, ST§2.4; as in the approach of [31]). We time scaled the phylogeny using *treePL* [32] with the first known stratigraphic occurrence for all genera following a budding model of evolution, where the younger of the two daughter lineages dates the split [33] (ST§2.5; fossil ages determined from an exhaustive literature search of 550 references in ST§6).

(c) Shell features and landmarking

Seven *a priori* shell features were landmarked on the bivalve shell (figure 1; full details on landmarking in ST§3.1). The features that operate together to open and close the animal's two valves are as follows: the **toothbank** (the area at which two valves articulate), the **ligament groove** (the site hosting the proteinaceous ligament that joins the two valves) and the adductor muscles as characterized by the **muscle scars** (the imprints on the inner surface of the shell where the muscles attach). The ventral extent of the animal's viscera—primarily the digestive, respiratory, circulatory and reproductive systems—is marked by the **pallial line**. The area that houses the siphons when retracted is marked by the **pallial sinus**; its depth and shape give an indication of siphon size that reflects the depth at which the animal lives below the sediment-water interface [34]. The **exterior surface** captures the general shape of the animal's shell, which is hypothesized to reflect burrowing behaviour and substratum use [19,20,35]. Features were landmarked using 'Pick Points' in Meshlab [36] (figure 1). Gridded surface semi-landmarks for the toothbank and exterior surface were placed following the procedure of [27], which is analogous to the eigensurface method of [37] and attempts to capture shape variation relative to the axis of maximum growth. Landmark density can affect inference of modularity structure [38], so the number of landmarks used to describe each feature was selected using both qualitative assessment of shape complexity and testing the statistical power of landmark coverage following [39] (electronic supplementary material, figure S4).

(d) General shape variation, phylogenetic signal and ecomorphology

General patterns in shape variation among genera were determined by principal components analysis of landmarks aligned using generalized Procrustes analysis (GPA; ST§3.2). Phylogenetic signal in GPA-aligned landmarks was assessed by a generalized K statistic [40] (ST§3.3). All morphological analyses from this point on were conducted on phylogenetically corrected shape data (i.e. the residuals from a phylogenetic least-squares regression of landmarks, ST§3.3). Distinctiveness of morphology by substratum use and clade membership was determined first by a permutation-based analysis of variance ('permANOVA' [41]), then as differences in mean shapes following [41] and lastly as the proportion of genera closer to the mean shape of their assigned group than to the mean shape of other groups (ST§3.4).

(e) Testing hypotheses of modularity structure

The modularity structure was determined using the effect size of the 'covariance ratio' (Z_{CR} in [42]; ST§3.5) for four groupings of the data: (i) the entire family Veneridae, (ii) the two major subclades A and B (figure 2*c*; electronic supplementary material, figure S2), (iii) the four substratum uses and (iv) deep- and shallow-infaunal genera within clades A and B. The best-supported hypothesis of modularity structure was determined by comparing the effect sizes of modularity strength (i.e. the most negative Z_{CR}, noting any overlap in confidence intervals) and by effect size tests ($\hat{Z}_{12}$ tests [42]; ST§3.5). Effect size tests suggested limited statistical power for differentiating hypotheses for some groupings of data; in these instances, the hypothesis with the most negative Z_{CR} was used as the 'optimal hypothesis' following [42]. Other approaches to analysing modularity exist (e.g. [43,44]), and some provide results consistent with Z_{CR} on empirical data [10], but we use the covariance ratio approach to facilitate comparison with many studies in the discussion.

(f) Modularity strength, within-module integration and morphological disparity

For the optimal hypothesis of modularity in subclades and ecological groups, modularity strength across the entire body was characterized by its Z_{CR} value (see [42]); more negative values indicate stronger modularity and thus relatively weaker covariation of traits (landmarks) between modules. Disparity of the entire body was measured as the Procrustes variance of the shape data centred on the mean shape of each analytical group (*sensu* [45], ST§3.6). Within-module integration was calculated using 'relative eigenvalue variance' ([46]; see also [47,48]; ST§3.6). Disparity of individual modules for each ecology was also measured using Procrustes variance, but on shape data with landmarks aligned per module-group combination and normalized by the number of landmarks in the module.

3. Results

(a) Ecological and phylogenetic signal in the morphology of venerid genera

The mean venerid shape is a moderately inflated, subtrigonal shell with equal-sized adductor muscle scars, a trigonal toothbank anterior of the shell midline, and a pallial sinus extending approximately 25% of the length of the shell. Thirty-eight per cent of the total shape variation in this dataset is explained by the first three principal components ('PCs'; 95% of the total variation explained by the first 39 PCs). Along the first PC, shapes vary from anterior–posterior elongate shells with deeper pallial sinuses and small toothbanks further offset anteriorly from the dorsal–ventral axis, to more equilateral shells with shallower pallial sinuses and more centrally positioned, broader toothbanks (figure 2*a*). The second PC captures variation in the inflation, or convexity, of the shell, and in the size of the pallial sinus and adductor muscles. The third PC shows an anti-correlation of features from PC1; more equilateral shell shapes are

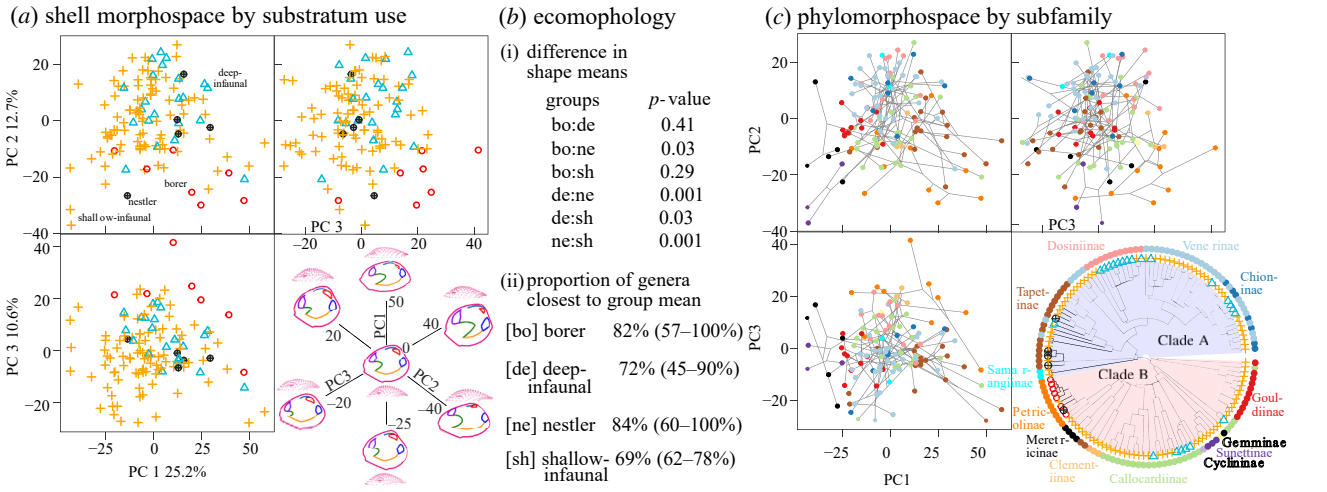

Figure 2. Morphological variation among 128 venerid genera. (*a*) Projections of genus morphology along the first three PCs, coloured by substratum use, with visualization of shape variation at specified scores along each axis (sagittal view also shown). (*b*.i) *p*-values for tests of differences in mean shape among substratum uses. (*b*.ii) Proportion of genera in each substratum use closest to the mean shape of their assigned substratum use with 95% confidence intervals. (*c*) The same PCs as in (*a*), but with points coloured by subfamily membership and connected by phylogenetic topology (substratum uses shown across tips of phylogeny with symbols as in (*a*); clades A and B after [24]; detailed phylogeny in electronic supplementary material, figure S2). (Online version is in colour.)

associated with offset, reduced area toothbanks and deep pallial sinuses, and elongate shells with more central, broader area toothbanks and shallower pallial sinuses.

Substratum use is broadly distributed across the first three PCs, with little evidence for distinct ecomorphologies at this low dimensionality (figure 2*a*). However, morphologies are significantly partitioned in morphospace by substratum use across the full-dimensional shape data while accounting for phylogeny (permANOVA $Z = 3.78$, $p = 0.001$), although not all mean shapes of substratum uses differ significantly from one another (i.e. borers compared to deep- and shallow-infauna, figure 2*b*). Up to 30% of genera within a substratum group are nearer to the mean shape of a substratum use other than their own, suggesting interfingering of morphospace occupation among subclades and life habits (figure 2*b*). While there is some ecological structure to the morphospace, phylogenetic signal is limited, indicating that sister-taxa are less similar in shape than expected under Brownian motion ($K_{\text{multi}} = 0.11$, $p = 0.002$). This is partially reflected in the phylomorphospace for PCs 1–3 (figure 2*c*), where sets of closely related taxa overlap in morphospace with more distantly related taxa (e.g. the Callocardiinae and Venerinae). Members of clades A and B are not significantly different in their morphology (permANOVA $Z = -6.78$, $p = 1$; see also electronic supplementary material, figure S5), further weakening phylogenetic signal in body shape.

(b) Modularity structure of the venerid shell

The optimal hypothesis of modularity structure across venerid genera is H2: shell versus internal anatomy (i.e. lowest Z_{CR}, figure 3*a*; values of Z_{CR}, *CR* and details of effect size tests, $\hat{Z}_{12}$, in electronic supplementary material, figure S6, ST§3.5). Each subclade and ecology is also optimally supported by H2 (figure 3*b*,*c*). For the two substratum uses that are shared across the subclades, shallow-infaunal genera from clades A and B are optimally supported by H2, as are the deep-infaunal genera from clade B. Deep-infaunal genera from clade A may have a more complex modularity structure H5, but the uncertainty in Z_{CR} overlaps with that of H2 (figure 3*c*). The Z_{CR} for H2 has non-overlapping confidence intervals with alternative hypotheses in 10 of 11 analytical groups (figure 3), but significant differences of pairwise effect size tests are mixed (i.e. $\hat{Z}_{12}$ tests). All alternative hypotheses are significantly different from the null hypothesis of no modularity at $p < 0.05$, but H2 is not significantly different from some other hypotheses in each analytical group (electronic supplementary material, figure S6). This uncertainty is mostly derived from the differences in the standard errors of *CR* estimated under the hypothesis of no modularity, such that Z_{CR} is most tightly estimated for H2 and more loosely estimated for the alternative hypotheses (electronic supplementary material, figure S6, ST§3.5). Because of H2's relatively tight estimate of Z_{CR}, and because its two-module parcellation of features is the most parsimonious hypothesis, H2 was treated as the optimal hypothesis of modularity structure for each analytical group.

(c) Modularity strength versus disparity

Disparity appears to increase with modularity strength between subclades and among substratum uses, but wide confidence intervals indicate uncertainty in this effect (figure 4*a*). Clade B has greater observed modularity strength and disparity than clade A, with no overlap in uncertainty of modularity strength and very small overlap in uncertainty of disparity (figure 4*a*). Among substratum uses, borers and shallow-infauna overlap in their uncertainties for modularity strength and disparity, but both appear to have greater observed modularity strength and disparity than nestlers and shallow-infauna, which overlap in their respective uncertainties. The wide uncertainty in the disparity of borers may derive from an interaction between their low sample size and high disparity. Differences in modularity strength should be interpreted using effect sizes (Z_{CR}), but *CR* values are useful for understanding degrees of modularity strength relative to no modularity ($CR = 1$). The *CR* for H2 across the family is 0.75 (electronic supplementary material, figure S6), which is a more tightly integrated structure than observed for other animals (e.g.

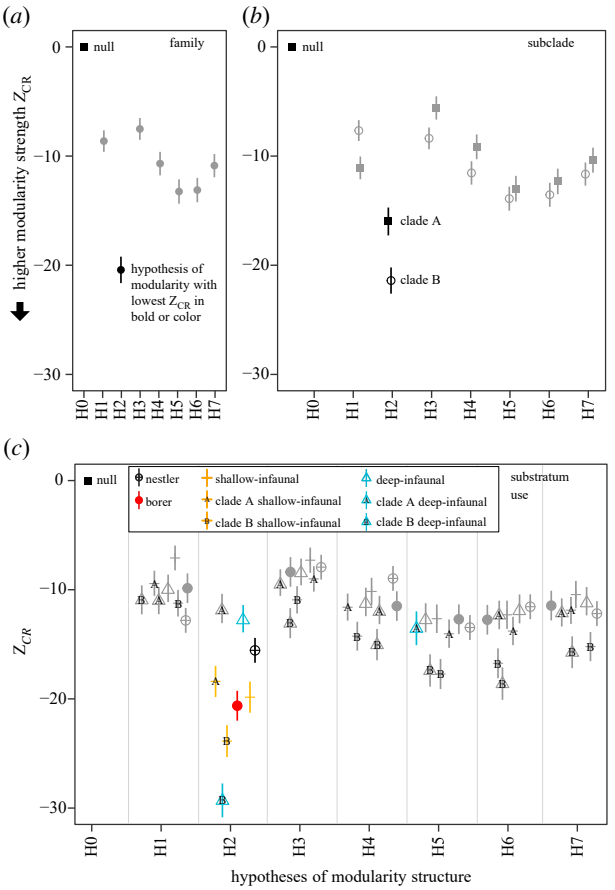

Figure 3. Support for hypotheses of modularity structure using the covariance ratio method. Points and ranges in panels are observed Z_{CR} scores with 95% confidence intervals. Non-grey points and intervals mark the hypothesis with lowest Z_{CR} per analytical group. (*a*) Optimal modularity structure across the family is H2 (i.e. the most negative Z_{CR}). (*b*) Subclades A and B are also optimally supported by H2. (*c*) H2 optimally supports the modularity structure of each substratum use, and H2 supports the structure of shallow- and deep-infaunal genera in clades A and B, excepting clade A deep-infauna that may be supported by a more complex structure (H5). Details on pairwise effects tests ($\hat{Z}_{12}$ tests of [42]) in electronic supplementary material, figure S6, ST§3.5. (Online version is in colour.)

mammal jaws [42]). *CR* values for subclades and substratum uses range between 0.6 and 0.9 (electronic supplementary material, figure S6). Qualitatively, the within-module disparity of analytical groups is not correlated with their within-module integration (i.e. covariation of their constituent landmarks; figure 4*b*).

4. Discussion

The morphology of a taxonomically diverse invertebrate clade, the bivalve family Veneridae—whose body plan is tied to an accretionary exoskeleton—has a stronger relationship to ecology than it does to phylogeny. This ecological differentiation, however, is not strictly linked to evolutionary shifts in the covariation of body features, and the operationally supported number of discrete modules falls well short of the hypothesized seven. Thus, for this clade, ecological and morphological diversification apparently occurred in only a couple of modules and rarely required changes in the covariation structure, reminiscent of patterns in the mammalian skull [49]. Even though the venerid body appears to be tightly integrated overall relative to elements of the vertebrate skeleton, its morphological disparity tends to increase with modularity strength among subclades and substratum uses. As discussed below, some of these results are consistent with findings in other animals and plants, but some may be unique to groups of animals having accretionary growth or to bivalves in particular.

(a) Distinct ecomorphologies with limited phylogenetic signal

With the exception of rock-boring genera, the morphology of venerids is partitioned to a first order by substratum use. The mean shape of rock-borers tends to resemble that of the deep- and shallow-infauna (figure 2*b*). Thus, the limited correlation between phylogeny and morphology may result from the multiple apparent origins of similarly shaped, deep-infaunal genera (figure 2*a*,*c*) and from the high disparity of shallow-infaunal genera, the ancestral state for the family ([50]; figures 2*a* and 4). Borers and nestlers tend to be phylogenetically clustered, which would increase the correlation between phylogeny and morphology (and morphology with ecology), but these phylogenetically localized effects are insufficient to create a strong signal across the entire family. Limited phylogenetic signal in morphology could be more a rule than an exception for bivalves, as evolutionary convergence of shell forms with similar functions has long been recognized [19,20]. Life near the sediment–water interface increases the risk of exposure to predators by wave or current action, so the shallow-infaunal body plan may be under selection for features related to stability in the substratum, anti-predatory defense and/or re-burrowing speed following displacement from their various substrata [20]. Similarly, life bored into rocks, deeply buried in sediment or nestled into crevices has been associated with distinctive morphologies, again reflecting selection for particular adaptations for those life modes. Boring animals carve into rocks harder than their calcium carbonate shells, with or without chemical aids [51]; deep-infaunal animals must penetrate more compacted sediment and maintain a longer conduit to the sediment–water interface than their shallow-infaunal relatives [19]; nestlers have some ability to adjust the growth of their shells to the shape of their enclosing cavities [52]. The diversity of adaptive demands on the venerid shell makes it even more striking that all four ecologies have the same modularity structure.

(b) Modularity structure: shell versus internal soft anatomy

The modularity structure is relatively simple across the family: features of the carbonate shell covary, and features reflecting the animal's internal soft anatomy covary. In retrospect, it may not be surprising that the bivalve shell, as opposed to the many elements in the vertebrate skeleton, imparts a simple covariation structure. The shell primarily grows by synchronous deposition of material along a continuous growth front [12], which could impose geometric restrictions for how the shell, and its toothbank and ligament, can change while maintaining the infaunal lifestyle of the family. We might expect even more extensive covariation of features, such that accretionary growth would regulate how the soft anatomy attaches to the shell. However, venerid body features are divided into two modules, one tied to the development of the shell ('shell': the toothbank, ligament

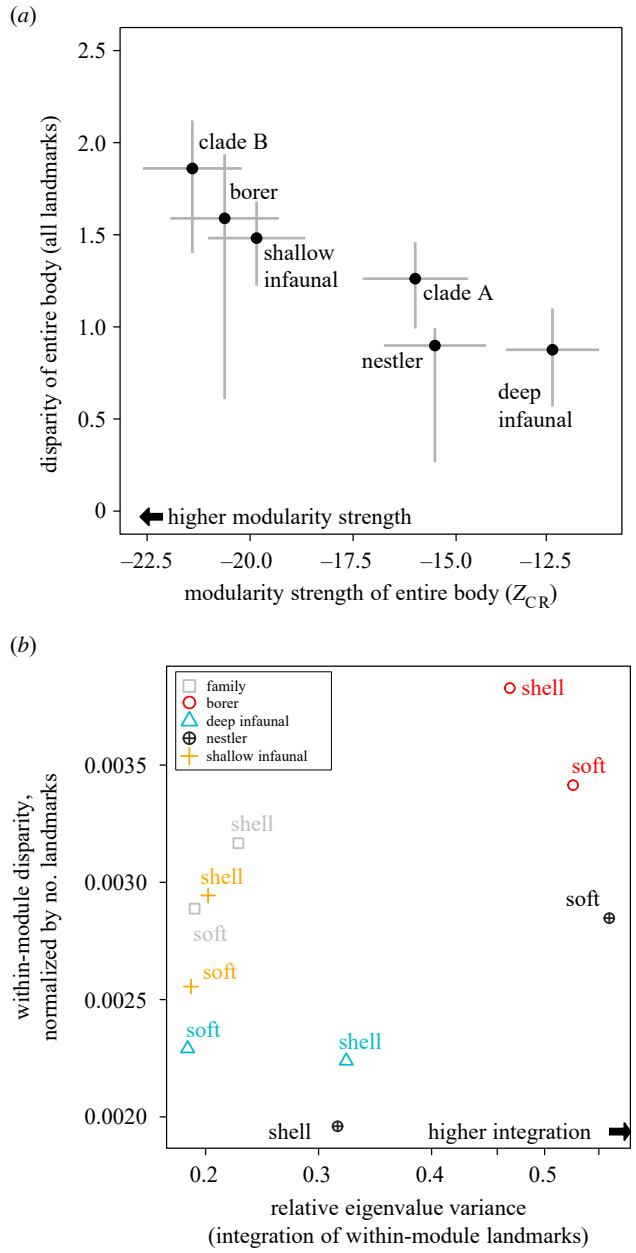

Figure 4. Comparing disparity to modularity strength and integration in the venerids for the two-module hypothesis of modularity structure (H2: shell versus internal anatomy). (*a*) Disparity of the entire body against modularity strength within substratum uses and subclades. Points mark mean values with line segments as 95% confidence intervals. (*b*) Within-module integration (i.e. covariance of a module's landmarks) against that module's disparity (compare relationships of modules within analytical groups). 'Shell' refers to the features forming the shell module and 'soft' refers to the features forming the internal soft anatomy module (see H2 in figure1). (Online version is in colour.)

and general shape of the shell's exterior surface) and the other reflecting the positions of the internal soft anatomy ('internal anatomy': the adductor muscle scars and the pallial line and sinus). Thus, the shapes of the shell and of the internal anatomy are less linked to one another as might have been expected from how the shell grows.

Division of features into modules representing the shell versus internal anatomy aligns more with the expectations of developmental integration than functional integration. Cell lineages that give rise to the shell separate very early in development from those that produce the adductor muscles and other parts of the animal's soft anatomy (possibly after two rounds of cell division [23,53]). Early separation of cell lineages does not preclude a later functional organization for these two modules. However, our analysis sorts features into those associated with the shell and those with the internal anatomy, suggesting that early development strongly imprints on the covariation of these features in adults. The ligament's grouping with the shell and toothbank also implies stronger developmental control because it is deposited by the mantle, like the shell (e.g. [54]). The 'shell' module could be functionally integrated, too; the animal's burrowing, boring and nestling mechanics require coordinated movement of the shell, toothbank and ligament in a lever system [55–57]. But, critically, the adductor muscles that close the shell during the burrowing sequence are part of the internal anatomy module; had they grouped with the features of the shell module, we might infer a relatively stronger control of function over development for the division of these two modules. We expected the boring habit to have strict morphological requirements that might drive the parcellation (*sensu* [1]) or restructuring of venerid modularity because the substratum, e.g. limestone, sandstone or even andesite [51], can be harder than the animal's carbonate shell. Even here, however, the modularity structure of the ancestral life habits is retained. Substratum use is the primary axis of ecological differentiation in venerids (all are mobile, unattached, suspension feeders [19,58]), but the covariation structure of venerid morphology appears to fall along mostly developmental lines, possibly reflecting successive steps in the evolution of the bivalve body plan. The internal anatomy and musculature attaching to the shell originated prior to the evolutionary origin of a functional hinge and ligament [59,60], although the homologs of the bivalve adductor muscles remain uncertain [61]. In this sense, venerids are perhaps more similar to the vertebrate skull, whose modules demonstrably have mixed origins in development, function and evolutionary sequence [25,62], than they are to organisms with individual modules strongly linked to discrete functions, such as flowering plants ([63] and references therein), dragonflies [64] and damselfishes [65].

The morphology of the venerid bivalve shell reflects more of the total anatomy of the animal than the skeletal elements considered in many of the vertebrate examples discussed above, which are mostly focused on cranial or vertebral elements in isolation. Still, the venerid bivalves have notably fewer modules than those vertebrates; for example, the two modules for venerids versus the six for the sigmodontine rodent mandible [42], six for the feeding system of aquatic foraging snakes [48], 10 for caecilian skull [10] and 16 for the frog cranium [25]). For that matter, venerids have fewer modules than most segmented animals (e.g. arthropods [66], with three modules in the cranidum of trilobites alone [67]). Further, the temporal conservation of this simple modularity structure considerably exceeds most vertebrate examples such as the mammalian skull [3,68,69], with the split between clade A and clade B dating back approximately 130 Myr. Thus, venerids show that evolution via many modules, or by restructuring modules, may not be as key to ecological diversification as it is for some plants or vertebrates [48,63,70]. This may reflect a macroevolutionary trade-off. The waiting time to evolutionary events that produce new ecologies could increase with decreasing module richness, even where taxonomic diversification rates are high as in this clade of approximately 750 extant species (although its diversification rate falls short of those in many vertebrate systems, e.g. [71]).

Recent analyses emphasize the rate of evolution for a module relative to the degree of integration of its components [8,63,72]. However, evolutionary transitions involving the separation of phenotypic elements into new modules can themselves promote an increase in a clade's rate and scope of morphospace occupation (e.g. [73] as cited above). Our venerid example provides a baseline, minimal number of modules for whole-organism comparative analyses. We suspect that other bivalve and invertebrate clades with more modules have evolved in morphospace at higher rates and to broader disparity than the venerids. See, for example, the extinct rudist bivalves, with their loss of bilateral symmetry and extensive alteration of musculature, hinge and ligament [6]; and see the irregular echinoids, with their many distinct phenotypic modules across their calcareous test [74].

(c) Stronger modularity, broader disparity?

In theory, broad morphological disparity can arise not only by modular evolution of body parts, but also by integrated evolution, or stronger covariance, of those parts. Some vertebrates show evidence of high disparity and strong integration [8,9], but the generality of this phenomenon is unclear (see lower disparity with higher integration in [8,75] and no relationship in [10,26,48,70]). In venerids, we find evidence for increasing disparity with decreasing integration (i.e. increasing modularity strength, figure 4*a*) and no evidence for a correlation between within-module integration and module disparity (figure 4*b*). A finer scale of modularity within the tissues, e.g. modules of gene expression within the mantle, may be sufficient to generate the remarkable range of shell form across Bivalvia and the Mollusca overall (e.g. [76]). At the same time, modularity and disparity may neither drive nor reflect taxon richness among venerid ecologies and subclades. For the most taxon-rich habit, living near the sediment–water interface, broad disparity is accompanied by relatively strong modularity (figure 4*a*), which we interpret as weaker covariation of the two modules (i.e. weaker integration). These patterns suggest that taxa have accumulated in a more isotropic manner than in the similarly rich deep-infaunal habit, which appears to have accumulated taxa more along evolutionary lines of least resistance—a more anisotropic array of morphologies (figure 4*a*). The taxon-poor boring or nestling habits are not restricted to particular corners of the modularity–disparity space, further weakening any link between disparity, modularity and diversity (figure 4*a*). These comparisons of modularity strength are relative, and overall, the venerid body is a tightly integrated structure (i.e. $CR = 0.75$ for the family, and ranging from 0.6–0.9 among subclades and substratum uses; electronic supplementary material, figure S6). Thus, origination along allometric trajectories, specifically heterochrony—a known developmental pathway for bivalve diversification [77–79]—may be a primary mode of taxonomic, ecological and morphological differentiation in venerids that maintains an evolutionary pattern of tight trait covariation. However, small shifts towards more mosaic evolution appear to increase morphological variance in certain subclades and ecologies. A true test of these dynamics will require comparisons with other major bivalve clades in an ontogenetic context. Nevertheless, the results here suggest that modularity strength is linked to disparity in this group of bivalves, but it is not clearly tied to evolutionary success in bivalves as measured by net diversification.

5. Conclusion

Overall, the disparity of the venerid bivalve clade is mostly underlain by two phenotypic modules, a split that appears to reflect developmental factors rather than functional ones. Even so, the net outcome of development, the adult body plan, is more strongly associated with ecology than with phylogeny, suggesting an unexplained ontogenetic role of the two major cell lineages that underlie the two modules [23]. The strength of modularity appears to be positively correlated with disparity among subclades and ecologies within this family. These morphological patterns suggest targets for developmental studies to determine the relative role of intrinsic and extrinsic factors in shaping the observed covariation (e.g. are the least disparate or most strongly integrated features developmentally more canalized under experimental manipulation? see [5]). They also provide a comparative basis for examining the developmental patterning and evolutionary impact of some of the more extreme deviations from the bivalve body plan, such as the loss of bilateral symmetry as in many scallops [16] and the extinct rudists [6], shifts of the visceropallium relative to the shell as in the giant clam *Tridacna* [80], repatterning of the musculature along the anterior–posterior axis as in oysters and mussels [81,82], and even the extreme elongation of extinct members of the venerids [28]. Given the phylogenetic and temporal breadth of this marine clade, extending this approach to other bivalve families and their extinct members will strengthen our understanding of how modularity and integration correspond to the differential accumulation of disparity and taxa in a morphology-rich clade founded on a simple accretionary exoskeleton.

Data accessibility. Mesh models, landmark data and phylogenetic data are available from the Dryad Digital Repository: https://doi.org/10.5061/dryad.dncjsxm0s [83]. Code: https://doi.org/10.5281/zenodo.5765233.

The stratigraphic occurrence data are provided in electronic supplementary material [84].

Authors' contributions. S.M.E.: conceptualization, data curation, formal analysis, funding acquisition, investigation, methodology, project administration, resources, software, supervision, validation, visualization, writing—original draft, writing—review and editing; S.C.K.: data curation, methodology, writing—review and editing; K.S.C.: data curation, investigation, methodology, validation, visualization, writing—review and editing; N.M.A.C.: formal analysis, methodology, software, writing—review and editing; D.J.: conceptualization, data curation, funding acquisition, resources, writing—review and editing.

All authors gave final approval for publication and agreed to be held accountable for the work performed therein.

Competing interests. We declare we have no competing interests.

Funding. This research was supported by National Aeronautics and Space Administration (NNX16AJ34G), the National Science Foundation (EAR-0922156, EAR-2049627), the UChicago Center for Data and Computing (to D.J.) and NSF Doctoral Dissertation Improvement Grant (DEB-1501880 to S.M.E.).

Acknowledgements. We thank M. Foote and T. Gao for discussion on disparity; M. Zelditch, D. Adams and M. Collyer for advice on testing modularity; A. Sartori for taxonomic advice on fossil venerids; M. K. McNutt and D. Wolfe for their support during a crucial phase in the writing of this paper and three anonymous, constructive reviewers; remaining errors are of course our own. Computations conducted on the Smithsonian Institution High Performance Cluster (SI/HPC). We also thank the museums and their staff for access to the specimens used in this study (NMNH, FMNH, CAS, UF).

References

1. Wagner GP, Altenberg L. 1996 Perspective: complex adaptations and the evolution of evolvability. *Evolution* **50**, 967–976. (doi:10.1111/j.1558-5646.1996.tb02339.x)
2. Goswami A, Polly PD. 2010 The influence of modularity on cranial morphological disparity in Carnivora and Primates (Mammalia). *PLoS ONE* **5**, e9517. (doi:10.1371/journal.pone.0009517)
3. Goswami A, Smaers JB, Soligo C, Polly PD. 2014 The macroevolutionary consequences of phenotypic integration: from development to deep time. *Phil. Trans. R. Soc. B* **369**, 20130254. (doi:10.1098/rstb.2013.0254)
4. Larouche O, Cloutier R, Zelditch ML. 2015 Head, body and fins: patterns of morphological integration and modularity in fishes. *Evol. Biol.* **42**, 296–311. (doi:10.1007/s11692-015-9324-9)
5. Uller T, Moczek AP, Watson RA, Brakefield PM, Laland KN. 2018 Developmental bias and evolution: a regulatory network perspective. *Genetics* **209**, 949–966. (doi:10.1534/genetics.118.300995)
6. Jablonski D. 2020 Developmental bias, macroevolution, and the fossil record. *Evol. Dev.* **22**, 103–125. (doi:10.1111/ede.12313)
7. Pigliucci M. 2003 Phenotypic integration: studying the ecology and evolution of complex phenotypes. *Ecol. Lett.* **6**, 265–272. (doi:10.1046/j.1461-0248.2003.00428.x)
8. Felice RN, Randau M, Goswami A. 2018 A fly in a tube: macroevolutionary expectations for integrated phenotypes. *Evolution* **72**, 2580–2594. (doi:10.1111/evo.13608)
9. Randau M, Goswami A. 2017 Unravelling intravertebral integration, modularity and disparity in Felidae (Mammalia). *Evol. Dev.* **19**, 85–95. (doi:10.1111/ede.12218)
10. Bardua C, Wilkinson M, Gower DJ, Sherratt E, Goswami A. 2019 Morphological evolution and modularity of the caecilian skull. *BMC Evol. Biol.* **19**, 30. (doi:10.1186/s12862-018-1342-7)
11. Hall BK. 1999 *Evolutionary developmental biology*, 2nd edn. Dordrecht, Netherlands: Springer.
12. Marin F, Le Roy N, Marie B. 2012 The formation and mineralization of mollusk shell. *Front. Biosci. (Schol. Ed.)* **4**, 1099–1125. (doi:10.2741/s321)
13. Jablonski D. 2017 Approaches to macroevolution: 1. General concepts and origin of variation. *Evol. Biol.* **44**, 427–450. (doi:10.1007/s11692-017-9420-0)
14. Crame JA. 2020 Early Cenozoic evolution of the latitudinal diversity gradient. *Earth-Sci. Rev.* **202**, 103090. (doi:10.1016/j.earscirev.2020.103090)
15. Bieler R, Mikkelsen PM, Giribet G. 2013 Bivalvia—a discussion of known unknowns. *Am. Malacol. Bull.* **31**, 123–133. (doi:10.4003/006.031.0105)
16. Sherratt E, Serb JM, Adams DC. 2017 Rates of morphological evolution, asymmetry and morphological integration of shell shape in scallops. *BMC Evol. Biol.* **17**, 248. (doi:10.1186/s12862-017-1098-5)
17. Cheverud JM. 1996 Developmental integration and the evolution of pleiotropy. *Am. Zool.* **36**, 44–50. (doi:10.1093/icb/36.1.44)
18. Schumm M, Edie SM, Collins KS, Gómez-Bahamón V, Supriya K, White AE, Price TD, Jablonski D. 2019 Common latitudinal gradients in functional richness and functional evenness across marine and terrestrial systems. *Proc. R. Soc. B* **286**, 20190745. (doi:10.1098/rspb.2019.0745)
19. Stanley SM. 1970 Relation of shell form to life habits of the Bivalvia (Mollusca). *Geol. Soc. Am. Mem.* **125**, 1–282. (doi:10.1130/MEM125)
20. Stanley SM. 1981 Infaunal survival: alternative functions of shell ornamentation in the Bivalvia (Mollusca). *Paleobiology* **7**, 384–393. (doi:10.1017/s009483730000467x)
21. Seilacher A, Gishlick AD. 2014 *Morphodynamics*. Boca Raton, FL: CRC Press.
22. Klingenberg CP. 2014 Studying morphological integration and modularity at multiple levels: concepts and analysis. *Phil. Trans. R. Soc. B* **369**, 33–35. (doi:10.1098/rstb.2013.0249)
23. Wada H, Phuangphong S, Hashimoto N, Nagai K. 2020 Establishment of the novel bivalve body plan through modification of early developmental events in mollusks. *Evol. Dev.* **22**, 463–470. (doi:10.1111/ede.12334)
24. Mikkelsen PM, Bieler R, Kappner I, Rawlings TA. 2006 Phylogeny of Veneroidea (Mollusca: Bivalvia) based on morphology and molecules. *Zool. J. Linn. Soc.* **148**, 439–521. (doi:10.1111/j.1096-3642.2006.00262.x)
25. Bardua C, Fabre AC, Bon M, Das K, Stanley EL, Blackburn DC, Goswami A. 2020 Evolutionary integration of the frog cranium. *Evolution* **74**, 1200–1215. (doi:10.1111/evo.13984)
26. Watanabe A, Fabre A-C, Felice RN, Maisano JA, Müller J, Herrel A, Goswami A. 2019 Ecomorphological diversification in squamates from conserved pattern of cranial integration. *Proc. Natl Acad. Sci. USA* **116**, 14– 688–14 697. (doi:10.1073/pnas.1820967116)
27. Collins KS, Edie SM, Gao T, Bieler R, Jablonski D. 2019 Spatial filters of function and phylogeny determine morphological disparity with latitude. *PLoS ONE* **14**, e0221490. (doi:10.1371/journal.pone.0221490)
28. Collins KS, Edie SM, Jablonski D. 2020 Hinge and ecomorphology of *Legumen* Conrad, 1858 (Bivalvia, Veneridae), and the contraction of venerid morphospace following the end-Cretaceous extinction. *J. Paleontol.* **94**, 489–497. (doi:10.1017/jpa.2019.100)
29. Schlager S. 2017 Morpho and Rvcg—shape analysis in R: R-packages for geometric morphometrics, shape analysis and surface manipulations. In *Statistical shape and deformation analysis: methods, implementation and applications* (eds G Zheng, S Li, G Székely), pp. 217–256. London, UK: Academic Press.
30. Bennett DJ, Hettling H, Silvestro D, Zizka A, Bacon CD, Faurby S, Vos RA, Antonelli A. 2018 Phylotar: an automated pipeline for retrieving orthologous DNA sequences from GenBank in R. *Life* **8**, 20. doi:10.3390/life8020020)
31. Soul LC, Friedman M. 2015 Taxonomy and phylogeny can yield comparable results in comparative paleontological analyses. *Syst. Biol.* **64**, 608–620. (doi:10.1093/sysbio/syv015)
32. Smith SA, O'Meara BC. 2012 TreePL: divergence time estimation using penalized likelihood for large phylogenies. *Bioinformatics* **28**, 2689–2690. (doi:10.1093/bioinformatics/bts492)
33. Crouch NMA, Edie SM, Collins KS, Bieler R, Jablonski D. 2021 Calibrating phylogenies assuming bifurcation or budding alters inferred macroevolutionary dynamics in a densely sampled phylogeny of bivalve families. *Proc. R. Soc. B* **288**, 20212178. (doi:10.1098/rspb.2021.2178)
34. Kondo Y. 1987 Burrowing depth of infaunal bivalves: observation of living species and its relation to shell morphology. *Trans. Proc. Paleontol. Soc. Jpn.* **1987**, 306–323. (doi:10.14825/prpsj1951.1987.148_306)
35. Stanley SM. 1975 Why clams have the shape they have: an experimental analysis of burrowing. *Paleobiology* **1**, 48–58. (doi:10.1017/S0094837300002189)
36. Visual Computing Lab ISTI – CNR. 2019 Meshlab.
37. Polly PD, MacLeod N. 2008 Locomotion in fossil Carnivora: an application of eigensurface analysis for morphometric comparison of 3D surfaces. *Palaeontol. Electron.* **11**, 10–13.
38. Goswami A, Watanabe A, Felice RN, Bardua C, Fabre A-C, Polly PD. 2019 High-density morphometric analysis of shape and integration: the good, the bad, and the not-really-a-problem. *Integr. Comp. Biol.* **59**, 669–683. (doi:10.1093/icb/icz120)
39. Watanabe A. 2018 How many landmarks are enough to characterize shape and size variation? *PLoS ONE* **13**, e0198341. (doi:10.1371/journal.pone.0198341)
40. Adams DC. 2014 A generalized K statistic for estimating phylogenetic signal from shape and other high-dimensional multivariate data. *Syst. Biol.* **63**, 685–697. (doi:10.1093/sysbio/syu030)
41. Collyer ML, Adams DC. 2018 RRPP: an R package for fitting linear models to high-dimensional data using residual randomization. *Methods Ecol. Evol.* **9**, 1772–1779. (doi:10.1111/2041-210X.13029)
42. Adams DC, Collyer ML. 2019 Comparing the strength of modular signal, and evaluating alternative modular hypotheses, using covariance ratio effect sizes with morphometric data. *Evolution* **73**, 2352–2367. (doi:10.1111/evo.13867)

43. Monteiro LR, Nogueira MR. 2010 Adaptive radiations, ecological specialization, and the evolutionary integration of complex morphological structures. *Evolution* **64**, 724–744. (doi:10.1111/j.1558-5646.2009.00857.x)
44. Goswami A, Finarelli JA. 2016 EMMLi: a maximum likelihood approach to the analysis of modularity. *Evolution* **70**, 1622–1637. (doi:10.1111/evo.12956)
45. Foote M. 1991 Morphological and taxonomic diversity in a clade's history: the blastoid record and stochastic simulations. *Contrib. Mus. Paleontol. Univ. Mich.* **28**, 101–140.
46. Pavlicev M, Cheverud JM, Wagner GP. 2009 Measuring morphological integration using eigenvalue variance. *Evol. Biol.* **36**, 157–170. (doi:10.1007/s11692-008-9042-7)
47. Machado FA, Hubbe A, Melo D, Porto A, Marroig G. 2019 Measuring the magnitude of morphological integration: the effect of differences in morphometric representations and the inclusion of size. *Evolution* **73**, 2518–2528. (doi:10.1111/evo.13864)
48. Rhoda D, Polly PD, Raxworthy C, Segall M. 2021 Morphological integration and modularity in the hyperkinetic feeding system of aquatic-foraging snakes. *Evolution* **75**, 56–72. (doi:10.1111/evo.14130)
49. Porto A, de Oliveira FB, Shirai LT, De Conto V, Marroig G. 2009 The evolution of modularity in the mammalian skull I: morphological integration patterns and magnitudes. *Evol. Biol.* **36**, 118–135. (doi:10.1007/s11692-008-9038-3)
50. Gardner RN. 2005 Middle-late Jurassic bivalves of the superfamily Veneroidea from New Zealand and New Caledonia. *N. Z. J. Geol. Geophys.* **48**, 325–376. (doi:10.1080/00288306.2005.9515119)
51. Kleemann K. 1996 Biocorrosion by bivalves. *Mar. Ecol.* **17**, 145–158. (doi:10.1111/j.1439-0485.1996.tb00496.x)
52. Yonge CM. 1958 Observations on *Petricola carditoides* (Conrad). *J. Molluscan Stud.* **33**, 25–31. (doi:10.1093/oxfordjournals.mollus.a064796)
53. Kurita Y, Hashimoto N, Wada H. 2016 Evolution of the Molluscan body plan: the case of the anterior adductor muscle of bivalves. *Biol. J. Linn. Soc.* **119**, 420–429. (doi:10.1111/bij.12812)
54. Waller TR. 1990 The evolution of ligament systems in the Bivalvia. In *The Bivalvia* (ed. B Morton), pp. 49–71. Hong Kong: Hong Kong University Press.
55. Ansell AD. 1962 Observations on burrowing in the Veneridae (Eulamellibranchia). *Biol. Bull.* **123**, 521–530. (doi:10.2307/1539573)
56. Coen LD. 1985 Shear resistance in two bivalve molluscs: role of hinges and interdigitating margins. *J. Zool.* **205**, 479–487. (doi:10.1111/j.1469-7998.1985.tb03539.x)
57. Ansell AD, Nair NB. 1969 A comparative study of bivalves which bore mainly by mechanical means. *Am. Zool.* **9**, 857–868. (doi:10.1093/icb/9.3.857)
58. Huber M. 2010 *Compendium of bivalves*. Harxheim, Germany: ConchBooks.
59. Pojeta J Jr, Runnegar B. 1985 The early evolution of diasome molluscs. In *The Mollusca, vol. 10, evolution* (eds ER Trueman, MR Clarke), pp. 295–336. Boston, MA: Academic Press.
60. Peel JS. 2021 Pseudomyona from the Cambrian of North Greenland (Laurentia) and the early evolution of bivalved molluscs. *Bull. Geosci.* **92**, 195–215. (doi:10.3140/bull.geosci.1827)
61. Waller TR. 1998 Origin of the molluscan class bivalvia and a phylogeny of major groups. In *Bivalves: an eon of evolution* (eds P Johnston, JW Haggart), pp. 1–45. Calgary, Canada: University of Calgary Press.
62. Fabre A, Dowling C, Portela Miguez R, Fernandez V, Noirault E, Goswami A. 2021 Functional constraints during development limit jaw shape evolution in marsupials. *Proc. R. Soc. B* **288**, 20210319. (doi:10.1098/rspb.2021.0319)
63. Dellinger AS *et al.* 2019 Modularity increases rate of floral evolution and adaptive success for functionally specialized pollination systems. *Commun. Biol.* **2**, 453. (doi:10.1038/s42003-019-0697-7)
64. Blanke A. 2018 Analysis of modularity and integration suggests evolution of dragonfly wing venation mainly in response to functional demands. *J. R. Soc. Interface* **15**, 20180277. (doi:10.1098/rsif.2018.0277)
65. Frédérich B, Olivier D, Litsios G, Alfaro ME, Parmentier E. 2014 Trait decoupling promotes evolutionary diversification of the trophic and acoustic system of damselfishes. *Proc. R. Soc. B* **281**, 20141047. (doi:10.1098/rspb.2014.1047)
66. Chipman AD, Edgecombe GD. 2019 Developing an integrated understanding of the evolution of arthropod segmentation using fossils and evo-devo. *Proc. R. Soc. B* **286**, 20191881. (doi:10.1098/rspb.2019.1881)
67. Webster M, Zelditch ML. 2011 Modularity of a Cambrian ptychoparioid trilobite cranidium. *Evol. Dev.* **13**, 96–109. (doi:10.1111/j.1525-142X.2010.00459.x)
68. Klingenberg CP. 2013 Cranial integration and modularity: insights into evolution and development from morphometric data. *Hystrix* **24**, 43–58. (doi:10.4404/hystrix-24.1-6367)
69. Hoffman EA, Rowe TB. 2018 Jurassic stem-mammal perinates and the origin of mammalian reproduction and growth. *Nature* **561**, 104–108. (doi:10.1038/s41586-018-0441-3)
70. Fabre AC *et al*. 2020 Metamorphosis shapes cranial diversity and rate of evolution in salamanders. *Nat. Ecol. Evol.* **4**, 1129–1140. (doi:10.1038/s41559-020-1225-3)
71. Felice RN, Goswami A. 2018 Developmental origins of mosaic evolution in the avian cranium. *Proc. Natl Acad. Sci. USA* **115**, 555–560. (doi:10.1073/pnas.1716437115)
72. Larouche O, Zelditch ML, Cloutier R. 2018 Modularity promotes morphological divergence in ray-finned fishes. *Sci. Rep.* **8**, 7278. (doi:10.1038/s41598-018-25715-y)
73. Young NM, Wagner GP, Hallgrímsson B. 2010 Development and the evolvability of human limbs. *Proc. Natl Acad. Sci. USA* **107**, 3400–3405. (doi:10.1073/pnas.0911856107)
74. Saucède T, Laffont R, Labruère C, Jebrane A, François E, Eble GJ, David B. 2015 Empirical and theoretical study of atelostomate (Echinoidea, Echinodermata) plate architecture: using graph analysis to reveal structural constraints. *Paleobiology* **41**, 436–459. (doi:10.1017/pab.2015.7)
75. Mitchell MJ, Goswami A, Felice RN. 2021 Cranial integration in the ring-necked parakeet, *Psittacula krameri* (Psittaciformes: Psittaculidae). *Biol. J. Linn. Soc.* **133**, 47–56. (doi:10.1093/biolinnean/blab032)
76. Herlitze I, Marie B, Marin F, Jackson DJ. 2018 Molecular modularity and asymmetry of the molluscan mantle revealed by a gene expression atlas. *GigaScience* **7**, 1–15. (doi:10.1093/gigascience/giy056)
77. Gould SJ. 1977 *Ontogeny and phylogeny*. Cambridge, MA: Harvard University Press.
78. Collins KS, Crampton JS, Neil HL, Smith EGC, Gazley MF, Hannah M. 2016 Anchors and snorkels: heterochrony, development and form in functionally constrained fossil crassatellid bivalves. *Paleobiology* **42**, 305–316. (doi:10.1017/pab.2015.48)
79. Pérez DE. 2019 Phylogenetic relationships of the family Carditidae (Bivalvia: Archiheterodonta). *J. Syst. Palaeontol.* **17**, 1359–1395. (doi:10.1080/14772019.2018.1532463)
80. Yonge CM. 1981 Functional morphology and evolution in the Tridacnidae (Mollusca: Bivalvia: Cardiacea). *Rec. Aust. Mus.* **33**, 735–777. (doi:10.3853/j.0067-1975.33.1981.196)
81. Yonge CM. 1954 The monomyarian condition in the Lamellibranchia. *Trans. R. Soc. Edinb.* **62**, 443–478. (doi:10.1017/S0080456800009352)
82. Yonge CM, Campbell JI. 1968 On the heteromyarian condition in the Bivalvia with special reference to *Dreissena polymorpha* and certain Mytilacea. *Trans. R. Soc. Edinb.* **68**, 21–42. (doi:10.1017/S0080456800014502)
83. Edie SM, Khouja SC, Collins KS, Crouch NMA, Jablonski D. 2021 Data from: Evolutionary modularity, integration and disparity in an accretionary skeleton: analysis of venerid Bivalvia. Dryad Digital Repository. (doi:10.5061/dryad.dncjsxm0s)
84. Edie SM, Khouja SC, Collins KS, Crouch NMA, Jablonski D. 2021 Evolutionary modularity, integration and disparity in an accretionary skeleton: analysis of venerid Bivalvia. Figshare.